

Numerical Study of Flame Acceleration in Microchannel

A. Chaudhuri, C. Guha and T. K. Dutta

Department of Chemical Engineering
Jadavpur University, Kolkata -700032

arnab_chaudhuri74@yahoo.co.in, cguhapaper@yahoo.com, proftapas_dutta@yahoo.com.

ABSTRACT

Phenomenon of flame acceleration of premixed combustible air-acetylene mixture towards the open end of adiabatic microchannel has been studied by solving Navier-Stokes (NS) system of equations with single step chemistry model. A two dimensional unsteady reactive NS solver has been developed using modified upwind splitting methods (AUSM+) and second order Runge-Kutta method to achieve the unsteady solutions. The predicted mechanism of flame acceleration, flame propagation speed and maximum outflow velocities are well in agreement with the conclusion drawn in the available literature related to the maximum flame acceleration configuration of the adiabatic microchannel.

Keywords: AUSM+, Combustion, Flame propagation, Microchannel, Micropropulsion.

1 INTRODUCTION

Microengineering and microelectronics processing technology have become potential research area due to the recent development of various cost effective and efficient microdevices. Optimal designs of Microelectromechanical systems (MEMS), nanoelectromechanical systems (NEMS) are need of the hour. Microcombustors, microburners, microactuators etc. are critical components of power MEMS devices. Due to the inherent complexity of the fluid dynamics in the micrometer scale, experimental and numerical studies have been proposed for better understanding of the physics of the microsystems. Limited work has been carried out on simulation of reacting flow in microcombustors. Norton and Vlachos [1, 2] studied methane-air and propane-air combustion characteristics and flame stability in microburners. Hua et al. [3, 4] studied the combustion characteristics of hydrogen-air mixture in microcombustors. Li et al. [5] predicted flame temperature of premixed flame taking hydrogen as fuel. Understanding of behavior of flame propagation, deflagration to detonation transition (DDT) in microchannels is typically important for the design of micropropulsion devices, ultra-micro gas turbines and other micro power systems. Ott et al. [6] predicted mechanism of laminar flame acceleration of acetylene-air system in narrow channel. Gamezo & Oran [7] extended their previous work [6] of flame acceleration related to micropropulsion application. Xu and Yu [8]

developed a slip model for species concentration to consider the rarefied gas effect at the boundary in microscale reactors and nanoscale structures. Kolb and Hessel [9] investigated diverse gas-phase reactions in microreactors, among them (partial) oxidations, hydrogenations, dehydrogenations, dehydrations, and reforming processes.

In this work, the phenomenon of flame acceleration of premixed combustible air-acetylene mixture towards the open end of adiabatic microchannel has been studied by solving Navier-Stokes (NS) system of equations with single step chemistry model. A two dimensional unsteady reactive NS solver has been developed to achieve the unsteady solutions. Modified upwind splitting methods (AUSM+) for convective flux and second order Runge-Kutta method have been utilized for simulation of microscale flame propagation. The non-reactive module of the developed code has been validated in our previous works [10-12] and high speed combustion characteristics of premixed stoichiometric air-acetylene mixture inside microchannels has also been studied [13]. This work is aimed at to study the flame propagation in microchannel to validate the developed unsteady reactive NS solver.

2 PROBLEM DESCRIPTION

The length (L: y axis), height (H: z axis) of the 2D microchannel are 1cm and 600 μm respectively with left end closed and right end open. The flame is initiated by a planar discontinuity in temperature and density located 366 μm from the closed end. The burned and unburned materials are considered to the left and right of the discontinuity respectively. The chemical reactions of acetylene-air mixture are considered as single step first order kinetics as mentioned in [6, 7]. The initial conditions and other physical properties and reaction parameters are taken similar to those presented in [6, 7]. Table 1 summarizes the conditions taken for simulation. The kinematic viscosity, diffusivity and thermal conductivity are calculated from $\nu = \nu_0 T^n / \rho$, $D = D_0 T^n / \rho$ and $k / (\rho C_p) = k_0 T^n / \rho$ with $n=0.7$.

3 NUMERICAL METHODS

Finite volume discretization of the reactive NS system of equations for compressible flow yields a set of algebraic equations that can be solved either by explicit or implicit method. Body fitted structured grids have been generated

using algebraic mapping with boundary refinement to solve the discretized equations. The convective fluxes and pressure terms are calculated using modified advection upwind splitting method (AUSM+) [14, 15] at a cell interface. The diffusive fluxes are calculated using central-average representations at the interface. The source terms for momentum and energy equations are functions of viscosity and velocity gradients. These are calculated by the product of the mean value of the integrand at the control volume (CV) centre and volume of the CV. The second order Runge-Kutta method consists of two steps. The first step can be regarded as half-step predictor based on explicit Euler method followed by midpoint corrector as given by equation 1.

$$\left. \begin{aligned} \phi_{n+1/2}^* &= \phi^n + f(t_n, \phi^n) 0.5\Delta t \\ \phi^{n+1} &= \phi^n + f(t_{n+1/2}, \phi_{n+1/2}^*) \Delta t \end{aligned} \right\} \quad (1)$$

where ϕ is the solution vector and superscript “n” denotes the time level of iteration.

The finite volume solver relies on the accuracy and robustness of AUSM+ and second order time accuracy of Runge-Kutta method. Since the geometry is symmetric about the axis half of the physical domain is considered as computational domain. Symmetry and adiabatic wall conditions are applied accordingly.

4 RESULTS AND DISCUSSIONS

It can be seen from Fig. 1 that there exists no significant variation of flame position (centerline) with time for 400×15 and 600×15 number of computational meshes. The results presented in this paper are based on 600×15 number of grids. The flame position is defined as the location in the flame front where the temperature is 1000K. Fig. 2 depicts the position of 2-D flame at the centerline and at the wall. It is evident from Fig. 3 that the centerline flame velocity increases with time while reaching the end of the microchannel. The velocity (y-component) variation with time is shown in Fig. 4. The velocity increases at the end of the microchannel as flow develops. The maximum outflow velocity reaches ≈ 138 m/s. Fig. 5 to 8 illustrate the development of temperature contours and boundary layer growth as initial planar flame starts to propagate down the channel. Fig. 9 and 10 show the product mass fraction and velocity (y-component) contours respectively at 0.000195 s. The boundary layer growth and burning of boundary layer material clearly reveal the phenomenon of flame acceleration in microchannel.

5 CONCLUSION

Gamezo and Oran [7] concluded that the maximum flame acceleration occurs when the channel height (640 μm) is about five times larger than the reaction zone of a laminar flame. We studied the flame acceleration in microchannel close to this aspect ratio. The developed solver is capable to predict the mechanism of flame acceleration, flame propagation speed and maximum outflow velocities. The results are well in agreement with the conclusion drawn in the given references related to the maximum flame acceleration configuration of the adiabatic microchannel.

6 ACKNOWLEDGEMENTS

This work has been carried out with the support of Senior Research Fellowship award from the Council of Scientific and Industrial Research (CSIR), India (9/96(4440)-2004-EMR-I). Furthermore, the authors would like to acknowledge the valuable suggestions received from Mr. Nilava Sen, Faculty, Dept. of Chem. Eng. Jadavpur University.

REFERENCES

- [1] D. G. Norton & D. G. Vlachos, *Chem. Eng. Sc.*, 58, 4871-4882, 2003.
- [2] D. G. Norton & D. G. Vlachos, *Combustion & Flame*, 138, 97-107, 2004.
- [3] J. Hua et al., *Chem. Eng. Sc.*, 60, 3497-3506, 2005.
- [4] J. Hua et al., *Chem. Eng. Sc.*, 60, 3507-3515, 2005.
- [5] Z. W. Li et al., *J. of Appl. Phys.*, 96, 3524-3530, 2004.
- [6] J. D. Ott et al., *AIAA J.*, 41, 1391-1396, 2003.
- [7] V. N. Gamezo & E. S. Oran, *AIAA J.* 44, 329-336, 2006.
- [8] B. Xu and Y. Ju, *AIAA 2004-304*, 42nd AIAA Aerospace Sciences Meeting and Exhibit, 2004.
- [9] G. Kolb and V. Hessel, *Chemical Engineering Journal*, 98, 1- 38, 2004.
- [10] A. Chaudhuri et al., *J. of Phys.: Conference Series*, IMEMS Conf., 34, 291-296, 2006.
- [11] A. Chaudhuri et al., *Chem. Eng. Technol.*, DOI: 10.1002/ceat.200600229, 2007.
- [12] A. Chaudhuri et al., *Chem. Eng. Technol.*, Accepted Dec 19th, 2006, ceat.200600366.
- [13] A. Chaudhuri et al., *Chem. Eng. Technol.*, Accepted Jan 9th, 2007, ceat.200600389.
- [14] M. S. Liou, C. J. Steffen(Jr.), *J. Comp. Phys.*, 107 23-39, 1993.
- [15] M. S. Liou, *J. Comp. Phys.*, 129, 364-382, 1996.

Property	Value
Temperature of unburned gas, T_o (K)	293
Temperature of burned gas, T_b (K)	2340
Initial pressure, P (N/m ²)	1.33×10^4
Specific heat ratio, γ	1.25
Molecular mass, M	29
Pre-exponential factor, A (m ³ /kg.s)	1×10^9
Activation energy, Q/R (K)	$29.3 T_o$
Chemical energy released, q	$35R T_o/M$
Transport constants, ν_o, D_o, k_o (kg/m.s.K ^{0.7})	1.3×10^{-7}

Table 1: Conditions for simulation

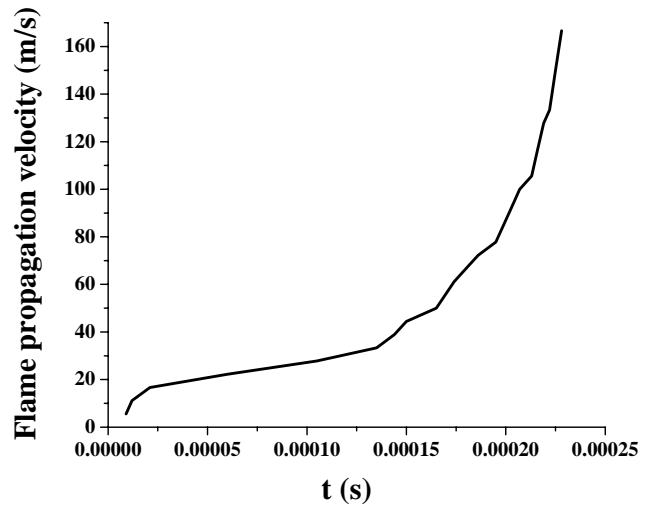


Figure 3: Flame propagation velocity

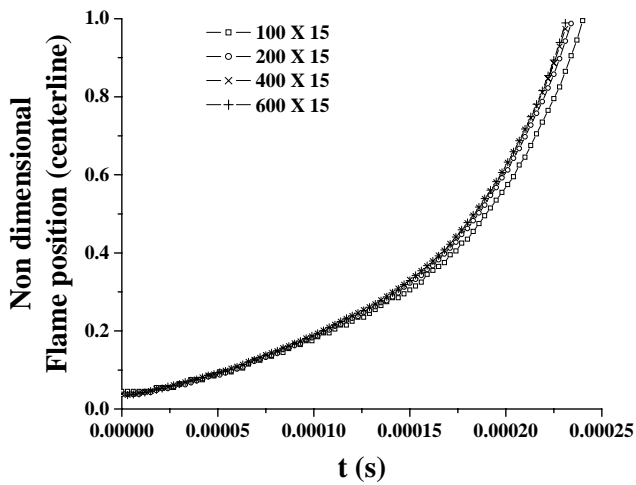


Figure 1: Grid study

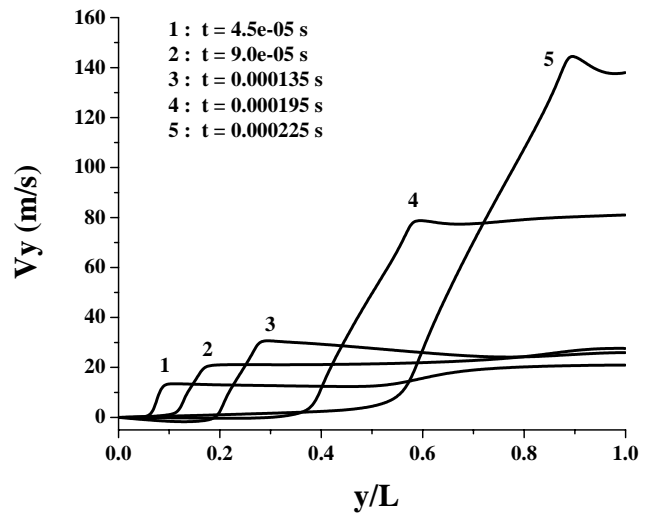


Figure 4: Time snaps of centerline velocity (V_y)

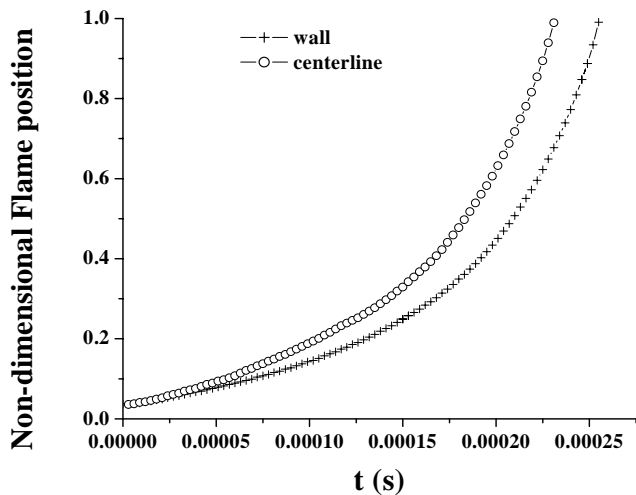


Figure 2: Flame position with time

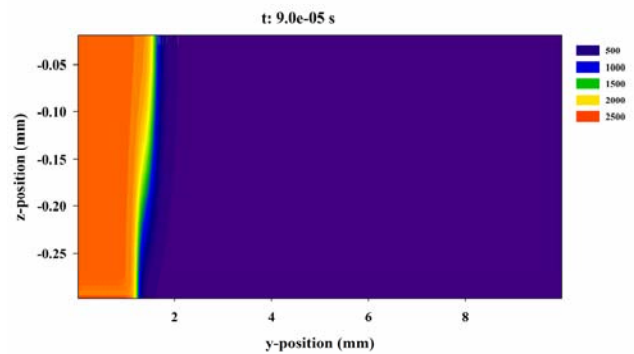


Figure 5: Temperature contour at $t: 9.0e-05$ sec

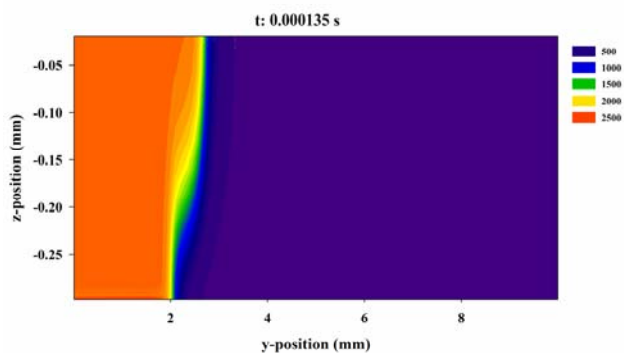


Figure 6: Temperature contour at t: 0.000135 sec

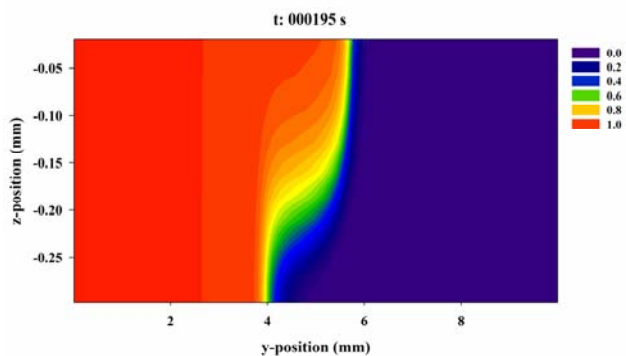


Figure 9: Product mass fraction contour at t: 0.000195 sec

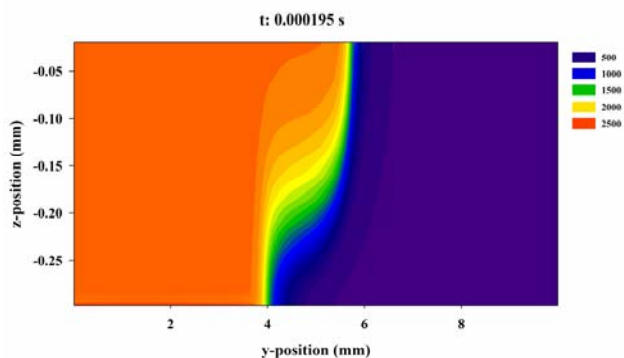


Figure 7: Temperature contour at t: 0.000195 sec

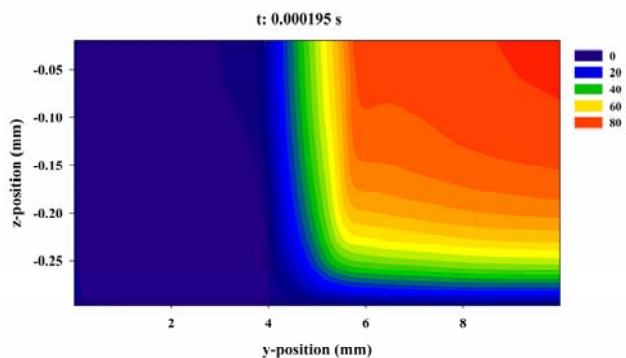


Figure 10: Velocity (V_y) contour at t: 0.000195 sec

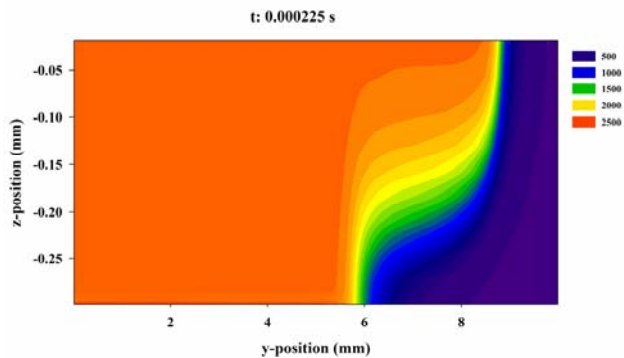


Figure 8: Temperature contour at t: 0.000225 sec